A Finite Integration Technique Based Simulation Study on the Impact of the Sternotomy Wires on the UWB Channel Characteristics

Mariella Särestöniemi[1], Carlos Pomalaza-Raez[2], Timo Kumpuniemi[1], Matti Hämäläinen[1], Jari Iinatti[1]

[1] Centre for Wireless Communications, University of Oulu, Finland
first name.familyname@oulu.fi

[2] Department of Electrical and Computer Engineering, Purdue University, USA

Abstract This paper presents for the first time a simulation study on the impact of the sternotomy wires on the ultra wideband (UWB) channel characteristics. The simulations are based on the finite integration technique (FIT). The simulation results are verified with the propagation path calculations as well as with the measurement data. It is found that there is a clear correspondence between the simulated and measurement results as well as with the propagation path calculations which allows smooth transceiver algorithm investigation.

Keywords: Electromagnetic propagation simulation, In-body Communication, Wireless Body Area Networks.

1 Introduction

Recently, in-body, or also called intra-body, communication has become intensively studied topic in the field on wireless body area networks (WBAN). Numerous channel models have been presented to describe the in-body channel characteristics [1]-[4]. Implant communication has also raised interest recently. Studies relating to the channel between the on-body antenna and the implant or between the implants have been under the scope [5]-[6]. However, the impact of the medical implants on the radio channel characteristics is scarcely studied topic. A study on the impact of the aortic valve implant on the channel characteristics was a pioneering work in this field, as shown in [7], which was later continued in [8]-[10].

Furthermore, medical wires, staples, and bands, which are used for the closure after the operation [11], can have significant impact since usually they are located close to the skin and hence close to the on-body antennas and sensor nodes. Besides, they usually contain titanium, steel, etc highly conductive material.

Impact of sternotomy wires on the UWB on-body channel characteristics was studied first time in [10] using measurement data based evaluations. It was shown that the sternotomy wires may cause additional peaks in the impulse response since the wires

form like loops which store and release energy to different directions. Besides, the signal may propagate faster via the wires.

The main contribution of this paper is to present, for the first time, a simulation based study on the impact of the sternotomy wires on the UWB radio channel characteristics and verify the simulation results with the measurement data and propagation calculations. The simulator is based on the finite integration technique (FIT), which is known to be among the best techniques in the propagation prediction in the vicinity of the human body [12]-[13]. After we can verify that the simulation is possible and model is satisfactory, it is possible to develop and investigate tranceiver's structures for in-body communications.

This paper is organized as follows: Section II describes the study case. Section III summarizes the calculated propagation paths. Section IV presents the numerical results. The summary and conclusion are given in Section V.

2 Study Case

2.1 Sternotomy wires

Sternotomy wiring is the most commonly used technique in the sternum closing after the operation that requires opening the sternum. The sternotomy wires are 1 mm wide, made from steel, and they are wrapped around the sternum, as shown in Figure 1. The distance between the sternotomy wires is approximately 2.5cm but it depends on the area of the sternum where the wires are located. [11]

Figure 1 illustrates also the location of the on-body antennas in this study. The transmitter antenna, Tx, is located in the left side of the sternum whereas the receiver antenna, Rx, is located in the middle of the sternum. The distance between the antennas is 15 cm. The distance between the antenna and the skin surface is 4 mm.

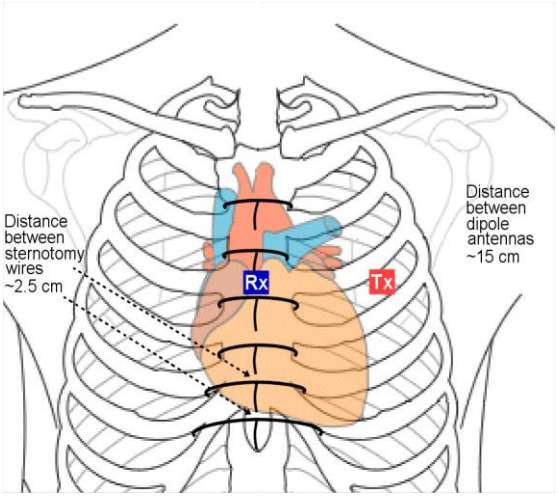

Fig. 1. Location of the sternotomy wires in the sternum.

2.2 Simulation model

In this study, a simplified layered human body tissue model has been used to evaluate the radio propagation in the vicinity and inside the human body. The layer model, presented in Figure 2, consists of the following tissues: skin, fat, muscle, bone, cartilage (cart.), heart, blood vessel, lung, and anterior mediastinum (ant. med). Due to simplicity, tissues are modeled as rectangular blocks. The dimensions of the tissues are designed according [4], as well as according to the x-ray figure of the implanted volunteer assisted in this study. The dielectric properties for different tissues were found in [16]. Furthermore, the sternotomy are modeled in the layer model. The layer model without the sternotomy wires, is used as a reference study case. Dipole antennas, which were presented for on- and off body communication in [14], were used in this study. The details of the antenna structure and radiation patterns are found in [14].

Simulations were conducted using the CST MicroWaveStudio (MWS) simulation software (CST) [15] for frequency bandwidth 0-10 GHz. Number of the samples within the simulated bandwidth was 2134. In this case, TX antenna is noted as Antenna 1 and RX antenna as Antenna 2. The simulator provides reflection coefficients S1,1 and S2,2, as well as channel responses S2,1 and S1,2 as an output. These results are then compared in the wire and non-wire cases, as well as verified with the measurement data.

2.3 Measurement Data

The aim of this study is to verify simulation results with measurement data presented in [10]. The details of the measurement scenario is explained in [10] and thus this section only briefly summarizes the measurement setup.

The measurements were taken in an anechoic chamber with two volunteers. One of them has sternotomy wires in his sternum. Besides, this volunteer has a titanium based aortic valve implant, which also has an impact on the channel characteristics as shown in [7],[10]. However, the time window, in which the impact of the aortic valve implant is visible (> 5ns), is out of the scope of this study and we merely focus on the time window where impact of the sternotomy wires is visible.

The measurements were conducted with Vector Network Analyzer (VNA) 8720ES in frequency domain to obtain channel frequency response (S21) and reflection coefficients S11 and S22. Frequency bandwidth used in the measurements was 3.1-10.6 GHz. Number of frequency points per sweep was set to 1601. Radio channel frequency response was then later transformed into time domain in Matlab using inverse fast fourier transform (IFFT) to get impulse response.

a)

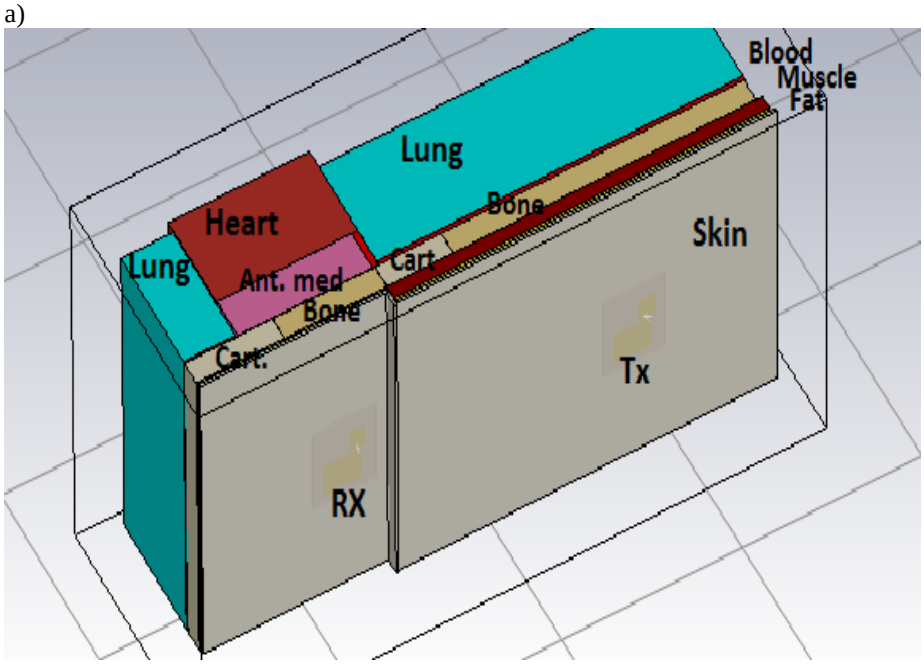

b)

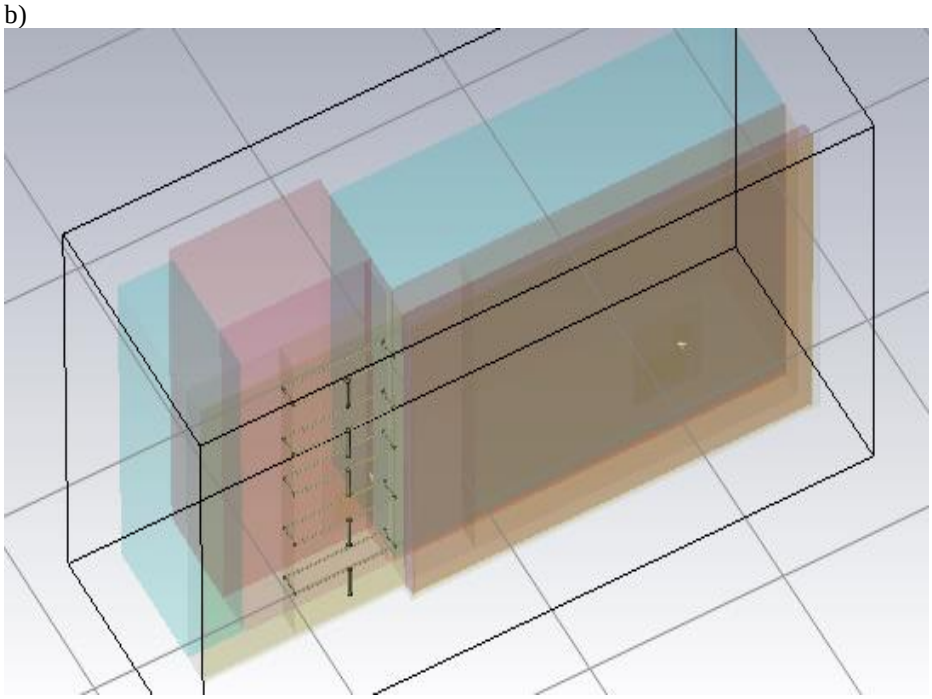

Fig. 2. Tissue layer models without (a) and with (b) the sternotomy wires.

3 Propagation Paths

In this section, different propagation path options are presented. The path options are calculated similar to [10] taking account the frequency, dielectric properties of the tissue and the distance travelled through the tissue. First, velocity of the propagation signal in the *i*th tissue is calculated as

$$v_{i,f} = \frac{c}{\sqrt{\varepsilon_{i,f}}}, \quad (1)$$

where $\varepsilon_{i,f}$ is the relative permittivity of a tissue at frequency *f*. This value, and also other dielectric properties of different tissues can be found e.g. in [16]. Table 1 summarizes $\varepsilon_{i,f}$ for the tissues used in the model. Once we know the velocity, we can easily calculate the propagation time in each of the tissues having a length of d_i using

$$t_{i,f} = \frac{d_i}{v_{i,f}}, \quad (2)$$

which are then summed up to obtain overall propagation time.

The propagation distance d_i may vary for tissues depending if it goes along the tissue or through the tissue. Propagation distance d_i:s are marked in the brackets for each propagation path options when it differs from the previous path's case.

In the presence of the wires, part of the signal may travel through wires which makes the propagation much faster. Besides, due their loop form, the wires absorb the energy and then release it afterwards in several directions. As explained in [10], this can be seen as additional or stronger peaks in the impulse responses. Furthermore, the sternotomy wires, which are located above or below the antenna, can have some impact as well since the propagating signal can be diffracted from the above/below –located wires towards the Rx antenna. Besides, the signal travels easily through the wires and their twisted ends so there will be summed up more signal energy than in the reference case.

The expected propagation paths within the tissue layer model are presented in Table 2. Since the idea of calculating the propagation paths is presented in [10], this paper just summarizes the path options.

Denotation bone/wire means that the signal travels through the bone and sternotomy wires in the simulation layer model with sternotomy wires. In the reference case, the signal travels through the bone. The calculated propagation times are summarized in Table 3. Denotations Path2 and Path2_w refer to the propagation path 2 in the reference case without sternotomy wires and with sternotomy wires, respectively.

Table 1. Relative permittivity for the tissues used in the layer model [16].

Tissue	2 GHz	4 GHz	6 GHz	8 GHz	10 GHz
Skin	38.6	36.6	34.9	33.2	37.5
Fat	5.32	5.12	4.94	4.76	4.6
Muscle	53.3	50.8	48.4	45.5	42.8
Lung	31.2	32.3	30.95	29.0	27.4
Anterior mediastenum	57.87	54.91	51.72	48.42	45.15
Blood vessel	59.0	55.7	52.5	48.61	45.11
Bone	19.6	16.95	15.2	13.83	12.61
Heart	58.8	52.0	52.2	45.37	42.24
Cartilage	39.8	35.6	31.8	28.47	25.63

Table 2. Propagation path options.

Path	Tissues and their dimensions within the path
Path 1	skin (15cm)
Path 2	skin (0.2cm)-fat (0.1cm)-muscle (0.6cm)-bone (rib, 1cm)-cartilage (2cm)-bone (sternum,1.5cm)/wire-fat (0.1cm)-skin (0.2cm)
Path 3	skin-fat-muscle-bone (rib,1cm)-blood (13.5cm)-bone (sternum, 1.5cm)/wire-fat-skin
Path 4	skin-fat-muscle (13.5cm)-bone sternum (1.5cm)wire-fat-skin
Path 5	skin-fat-muscle (11.5cm)-cartilage (2cm)-sternum bone/wire-fat-skin
Path 6	skin-fat-muscle-bone-lung (13.5cm)-anterior mediastinum (2cm)- bone (sternum)/wire-fat-skin
Path 7	skin-fat-muscle-bone-lung (13.7cm)-heart (2cm)-anterior mediastinum-bone (sternum)/wire-fat-skin

Table 3. Propagation times for propagation paths. Path2=reference, Path2w=wire case etc

Path/ frequency	2 GHz	4 GHz	6 GHz	8 GHz	10 GHz
Path 1	3.14 ns	3.06 ns	2.99 ns	2.94 ns	2.94 ns
Path 2	1.29 ns	1.26 ns	1.39ns	1.21 ns	1.20 ns
Path 2w	1.135ns	1.112 ns	1.2ns	1.07 ns	1.05ns
Path 3	3.30ns	3.20ns	3.20ns	3.02ns	2.94ns
Path3w	3.20ns	3.12ns	3.17ns	2.95ns	2.86ns
Path 4	3.527ns	3.45ns	3.507ns	3.294ns	3.22ns
Path4w	3.411ns	3.34ns	3.34ns	3.184ns	3.11ns
Path 5	3.462ns	3.34ns	3.424ns	3.205ns	3.12ns
Path5w	3.346ns	3.26ns	3.311ns	3.095ns	3.01ns
Path 6	3.501ns	3.40ns	3.458ns	3.235ns	3.15ns
Path6w	3.385ns	3.29ns	3.345ns	3.126ns	3.04ns
Path 7	4.0 ns	3.84ns	3.88 ns	3.64ns	3.55ns
Path 7 w	3.8ns	3.68ns	3.73 ns	3.5ns	3.51ns

4 Numerical Results

In this section, the simulation results are examined by comparing the wired and non-wired simulation model cases. The results are reflected to the propagation path options presented in the previous section. Furthermore, the results are verified with the measurement data.

At first, we compare the results in frequency domain. Figure 3a and 3b presents reflection coefficients S1,1 for antenna 1 (on the left side of the chest) and S2,2 for antenna 2 (in the middle of the sternum), respectively. The results obtained with the simulation model with sternotomy wires is marked as S1,1 or S2,2, and they are plotted as black curves. The reference case, i.e., the results obtained with the layer model without the sternotomy wires, is denoted as S1,1_1 and S2,2_1 and plotted as blue curves.

As it can be noticed from Figure 3a, there is no difference between the reflection coefficients S1,1 and S1,1_1, since the sternotomy wires are enough far away from the antenna 1 to have any impact on the reflection coefficient. Thus, the S1,1 and S1,1_1 curves are equal and they are completely overlapping. Instead, in the reflection coefficients of antenna 2, which is exactly above the sternotomy wires, one can notice a difference clearly, especially at frequency range 3-6 GHz.

Figure 4 presents the channel response for the wired (S2,1) and non-wired cases (S2,1_1). There is only some small differences in the lower part of the frequency range. However, despite of small changes in frequency domain, we can see more differences in time domain results presented in Figures 5-7. Figure 5-6 present the impulse response obtained by performing IFFT for the whole frequency bandwidth 0-10 GHz, up to 5 ns and up to 16 ns, respectively. Figure 7 presents the impulse response obtained by performing IFFT for the bandwidth 3.1-10.6 GHz, which corresponds to the bandwidth used in the measurements.

When comparing the impulse responses in Figure 5, we can notice that the main peaks are at the same level but there are changes in the following side peaks. The location of the peaks match well with the propagation path calculations presented in Table 2. According to the calculations, impact of the wires should be seen at time instants 1.3ns (Path 2), 2.6ns (Path), 3.5-4.0 ns (Path 7) which can be noted in the impulse response. In the case of Path 2, in the impulse response of the wired model has a peak starting slightly earlier than in the non-wired model (due to enhanced propagation time when signal travel via wires). Besides, the corresponding peak is at higher level with the wired model than with the non-wired model, since there will be summed more energy due to the impact of the wires above and below the antennas.

The time window 3.5-4.0 ns, which corresponds to Path option 7, is interesting: we can notice that there is a clear peak at this time range, much stronger than in the wired-model case. Normally the peaks are stronger when the wires are influencing. This may be due to the fact that the signal propagating through lungs until the heart and then to anterior mediastinum, is already strongly attenuated when reaching the wires. There might not be enough energy they could accumulate to release it afterwards, like in the Path 2's case. As explained earlier, the wired loops absorb the energy and then release it afterwards in several directions. In the case of Path 7, the released energy that is in the direction of the antenna, might be too weak to be recognized in the channel response. Figure 6 presents the impulse responses for the larger time range, up to 16 ns. There we can see the oscillating effect due to the wires at the lower dB levels.

.Next we compare the results with the measurement data. The impulse responses obtained from the measurements are presented in Figures 8a-b, for wire case and non-wire case, respectively. These two measured impulse response figures have already been presented in [10], but they are repeated in this paper to enable smooth comparison between the measurement and simulation results. One should note that the measurement data is obtained with the volunteer having also an aortic valve implant besides of the sternotomy wires. However, based on the propagation calculations presented in [10] we know the time window at which aortic valve effect appears, and thus we focus only the time window up to the aortic valve effect.

When comparing simulated IRs in Fig. 5 to measured IRs in Figs 8a and b, one can note that clear similarity in the shapes of the simulated and measured impulse responses since the locations of the sidepeaks respect to the main peak are similar. However, the delays due to the unidealities in the measurements, such as the delays due to the antennas etc.[17], should be taken into account. Instead, there is clear differencies in the level of the peaks, especially in the main peaks. In the simulated impulse responses, the mainpeak level is approximately at 55 dB and there is no difference between the wired

and non-wired case. With the measurement data, the level with wired model is around -62 dB and non-wired model -72 dB. The level difference is surprisingly high. Level differencies may be due to different body shapes, different antenna attachments, different clothing, unidealities in the antenna prototyping, etc.

As explained in the Section II, the measurement was conducted for the frequency band 3.1-10.6 GHz. Thus, it is relevant to compare measured impulse responses with Figure 7, in which IFFT was perfomed for the simulated channel response withihn the frequency range 3.1-10.6 GHz. We notice that in this case, the shapes of the simulated and measured impulse responses are even more similar, but only until 2 ns, after which the simulated impulse responses fades completely. Apparently, the resolution of the 7.5 GHz bandwidth with the selected simulation settings in not enough to show the peaks after 2 ns.

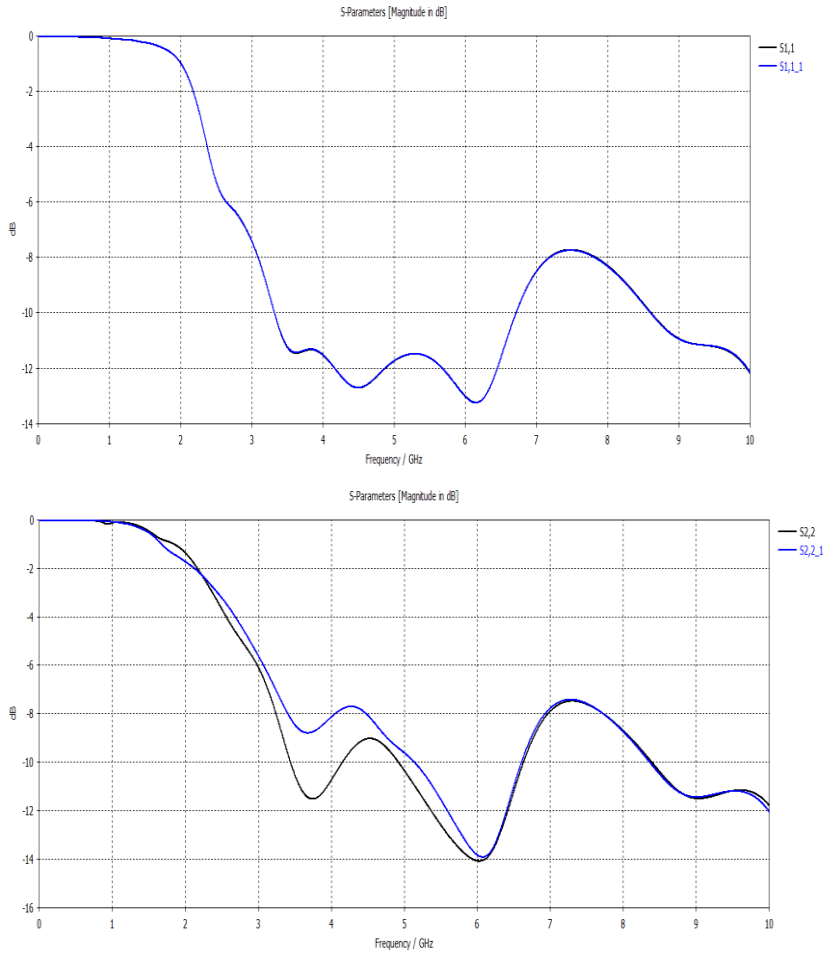

Fig. 3. a) Simulated reflection coefficients for antenna 1 with sternotomy wires (S1,1) and without the sternotomy wires (S1,1_1) and b) for antenna 2 with sternotomy wires (S2,2) and without the sternotomy wires (S2,2_1).

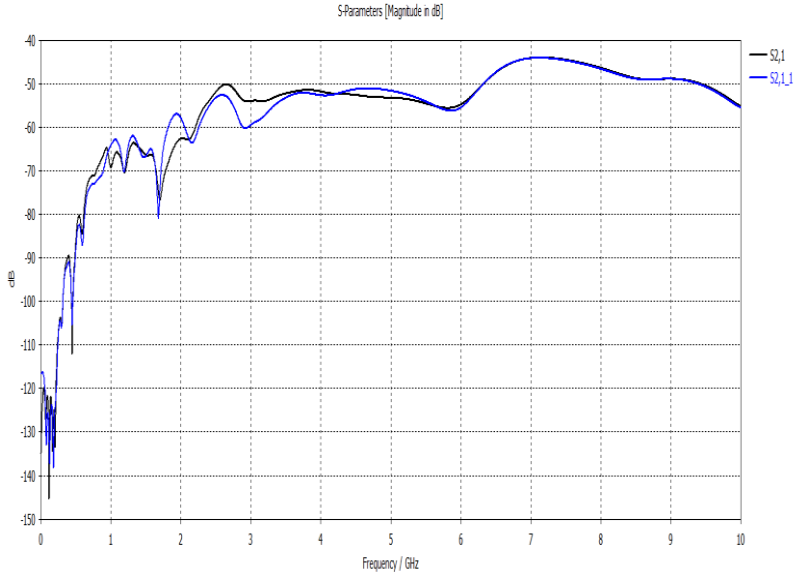

Fig. 4. Simulated channel parameter with sternotomy wires (S2,1) and without the sternotomy wires (S2,1_1).

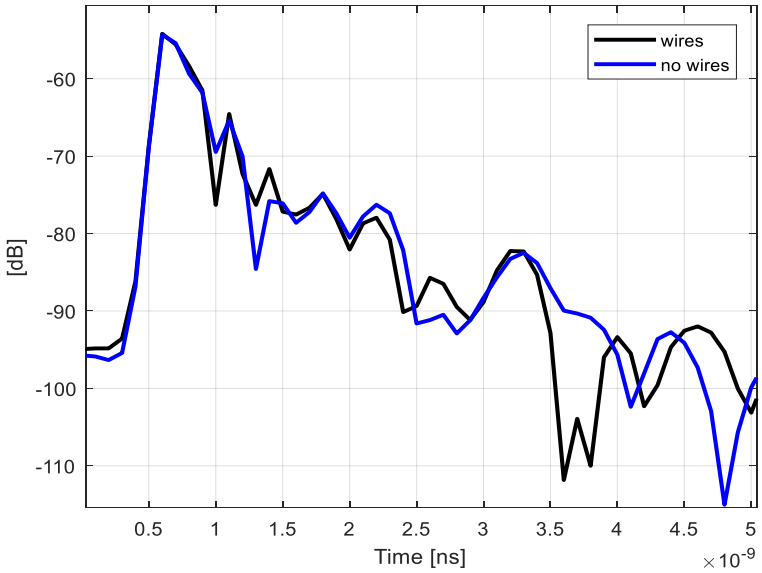

Fig. 5. Simulated impulse responses for wired and no wired cases as the IFFT is performed for 0-10 GHz, presented up to 5 ns.

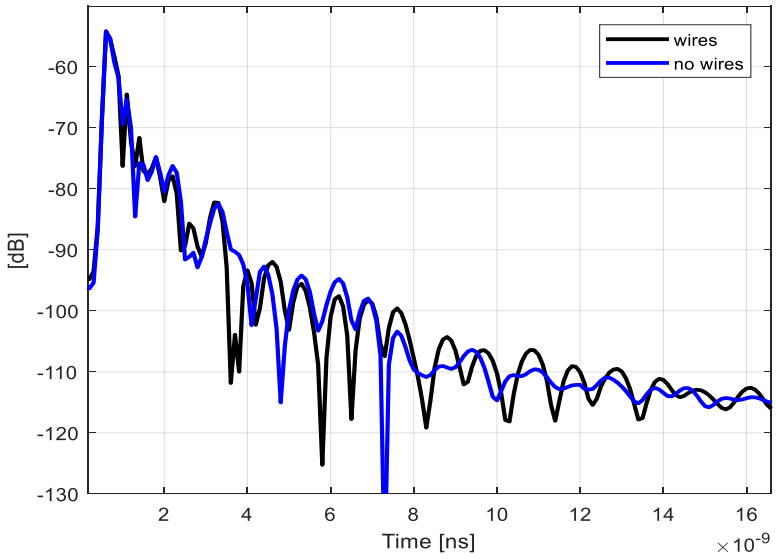

Fig. 6. Simulated impulse responses for wired and non-wired cases as the IFFT is performed for 0-10 GHz bandwidth, presented up to 16 ns.

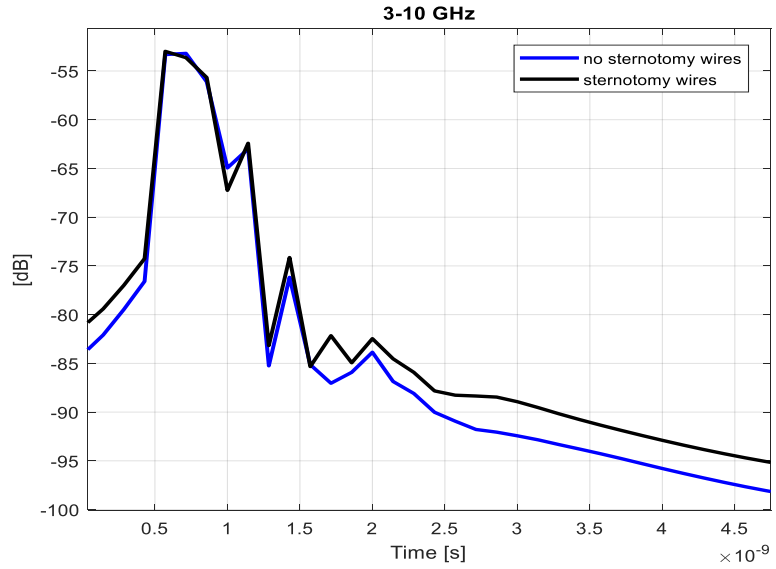

Fig. 7. Simulated impulse responses for wired and no wired cases as the IFFT is performed for 3-10 GHz bandwidth.

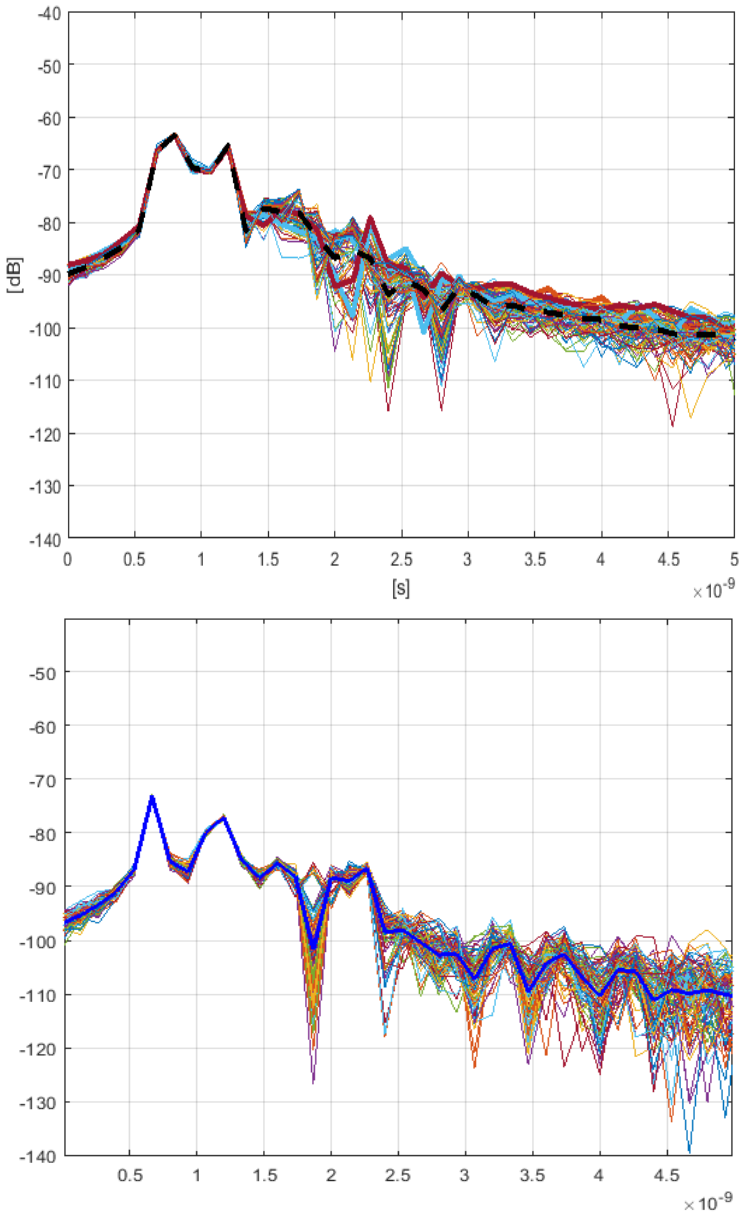

Fig. 8. Measured impulse responses a) with and b) without the wires [10].

5 Summary and Discussion

In this paper, we have presented FIT-based simulation study on the impact of the sternotomy wires on the UWB on-body channel characteristics. The results are verified with the measurement data and propagation path calculations. In the simulations, we used human tissue layer model, whose dimensions were designed taking into account the volunteers body size. It was found that there is a clear correspondence between simulated and measurement results. Besides, the location of the peaks in the simulated impulse response match well with the propagation path calculations.

The benefit of using a human tissue layer model in this kind of study is that we can design the layer model according to the dimensions of the volunteer. The implanted volunteer who assisted in our measurements, is lean and hence, and thus his fat tissue is very thin. Since the propagation loss in the fat tissue is high, the impact of the sternotomy wires is assumed to be clearer in the cases of lean people. Our next target is to study the impact of the body structure on sternotomy wire effect.

The knowledge about the impact of sternotomy wires on the channel characteristics is important because the additional peaks or stronger side peaks may cause some interference on the monitoring devices. It should be noted that in this study we used antennas designed for on- and off body communication. With antennas designed for in-body communication, (used for instance in the capsule endoscopy localization), the impact of the sternotomy wires is presumably even more significant, which belongs to our next research plan as well.

Acknowledgements

This research has been financially supported by the project WBAN Communications in the Congested Environments and in part by Academy of Finland 6GGenesis Flagship (grant 318927).

References

1. P. Turalchuk, I. Munina, V. Pleskachev, V. Kirillov, O. Vendik, I. Vendik, “In-Body and On-Body Wave Propagation: Modeling and Measurements,” *International workshop on Antenna Technology: Small Antennas, Innovative Structures, and Applicattions (iWAT)*, 2017.
2. N. R. Amon, I. Mahbub, P: Kanai. Saha, ”Propagation Characteristics of Ultra-Wideband Pulse in Multilayered Human Chest Tissue,” *International Conference on Electrical Engineering and Information Communication Technology (ICEEICT)*, 2016.
3. I. Dove, "Analysis of Radio Propagation Inside the Human Body for in-Body Localization Purposes", University of Twente, Netherland, Aug. 2014.
4. K. N. Sahu, C. D. Naidu, M. Satyam, K. Jaya Sankar, ”Study of RF Signal Attenuation of Human Heart,” Hindawi Journal on Engineering, 2015
5. J. Li, Z. Nie, Y. Liu, L. Wang, Y. Hao, ”Characterization of In-Body Radio Channels for Wireless Implants,” IEEE Sensors Journal, Vol. 17, No. 5, 2017.

6. C. Garcia-Pardo, A. Fornes-Leal, N. Cardona, S. Brovoll, o. Aardal, S.-E. Hamran, R. Chavez-Santiago, J. Berland, I. Balasingham, R. Palomar, “Experimental Ultra Wideband Path Loss Model for Implant Communication,” *IEEE International Symposium on Personal Indoor and Mobile Radio Communications (PIMRC)*, 2016
7. A. Taparugssanagorn, C. Pomalaza-Ráez, A. Isola, R. Tesi,M. Hämäläinen, J. Iinatti, ”UWB Channel Modeling for Wireless Body Area Networks in Medical Applications,” Applied Sciences in Biomedical and Communication Technologies (ISABEL), 2009
8. A. Taparugssanagorn, C. Pomalaza-Ráez, A. Isola, R. Tesi,M. Hämäläinen, J. Iinatti, "Preliminary UWB Channel Study for Wireless Body Area Networks in Medical Applications" in International Journal of Ultra Wideband Communications and Systems, InderScience Publishers, vol. 2, no. 1, pp. 14-22, 2011
9. W-B. Yang, K. Sayrafian-Pour, J. Hagedorn, J. Terrill, K.Y. Yazdandoost, A. Taparugssanagorn, M. Hämäläinen, J. Iinatti, "Impact of an Aortic Valve Implant on Body Surface UWB Propagation: A Preliminary Study", *Proc. the 5th International Symposium on Medical Information and Communication Technology*, 2011
10. M. Särestöniemi, T. Kumpuniemi, M. Hämäläinen, C. Pomalaza-Raez, J. Iinatti, ”Impact of the Sternotomy Wires and Aortic Valve Implant on the On-body UWB Radio Channel,” publish in ISMICT 2018, March 2018
11. A. Elfström, A. Grunditz, “Evaluation of Sternum Closure Techniques Using Finite Element Analysis, ” Master Thesis, in Medical Engineering, The Royal Institute of Technology, Sweden, 2013.
12. M. Särestöniemi, M. Hämäläinen, J. Iinatti, ”An Overview of Electromagnetic Propagation Based Channel Modeling Techniques for Wireless Body Area Network Applications,” IEEE Access, 2017.
13. A. Pellegrini, A. Brizzi, L. Zhang, K. Ali, Y. Hao, X. Wu, C. C. Constantinou, Y. Nechayev, P. S. Hall, N. Chahat, M. Zhadobov, R. Sauleau, "Antennas and Propagation for Body-Centric Wireless Communications at Millimeter-Wave Frequencies: A Review [Wireless Corner]", *Antennas and Propagation Magazine IEEE*, vol. 55, 2013
14. T. Tuovinen, K. Yekeh Yazdandoost, J. Iinatti, ”Comparison of the Performance of Two Different UWB Antennas for the use in WBAN On-Body Communications,” 6th Europ. Conf. Antennas and Propagation (EUCAP), 2012.
15. CST Microwave Studio, [Online]. Available: http://www.cst.com.
16. https://www.itis.ethz.ch/virtual-population/tissue-properties/database/dielectric-properties.
17. T. Kumpuniemi, T. Tuovinen, M. Hämäläinen, K. Yekeh Yazdandoost, R. Vuohtoniemi, J. Iinatti, "Measurement-Based On-Body Path Loss Modelling for UWB WBAN Communications", *The 7th International Symposium on Medical Information and Communication Technology (ISMICT2013)*, Tokyo, Japan, March 6-8, 2013.